

# Normalization of Experimental Modal Vectors to Remove Modal Vector Contamination

**A.W. Phillips, R.J. Allemang**

Structural Dynamics Research Laboratory  
Department of Mechanical and Materials Engineering  
College of Engineering and Applied Science  
University of Cincinnati  
Cincinnati, OH 45221-0072 USA  
**Email: Allyn.Phillips@UC.EDU**

## Abstract

When modal vectors are estimated from measured frequency response function (FRF) data, some amount of contamination in terms of random and bias errors is always present. The sources of these errors may be the experimental data acquisition process (calibration inconsistencies, averaging limitations, leakage errors, etc.) or due to limitations of the modal parameter estimation methods (mismatch between measured FRF data and the model form). These random and bias errors include uncertainty in complex magnitude about the central axis of the modal vector as well as rotation of the central axis. In a number of practical applications, particularly those involving close modal frequencies, the contamination of a modal vector will often have a significant influence from the modal vector that is near in frequency. In these situations, the numerical procedure for estimating the final, scaled modal vector, in terms of residue, generally involves a linear estimation method that, with MIMO FRF data, utilizes a weighted least squares solution procedure. This numerical solution process is reviewed and a real normalization of the weighting vectors used for estimating each modal vector in the MIMO FRF case is shown to reduce the contamination from nearby modal vectors. Theoretical evaluations for both proportional and non-proportional analytical cases are evaluated, as well as, results for a real application with pseudo-repeated modal frequencies and associated modal vectors that has historically demonstrated the problem.

**Keywords:** Residue Estimation, Modal Vector Contamination, Modal Participation Weighting, MAC, Modal Vector Estimation

## Nomenclature

$N_i$  = Number of inputs.

$N_o$  = Number of outputs.

$N_S$  = Short dimension size.

$N_L$  = Long dimension size

$\lambda_r$  = Complex modal frequency (rad/sec).

$\lambda_r = \sigma_r + j \omega_r$

$\sigma_r$  = Modal damping.

$\omega_r$  = Damped natural frequency.

$r$  = Mode number.

$\omega_i$  = Discrete frequency (rad/sec).

$[H(\omega_i)]$  = FRF matrix ( $N_o \times N_i$ ).

$A_{pqr}$  = Residue for response DOF p, input DOF q, mode r.

MAC = Modal assurance criterion.

riMAC = MAC (real versus imaginary).

riwMAC = Weighted MAC (real versus imaginary).

## 1. Introduction

As modal parameter estimation has evolved over the last forty years or so, the way that modal vectors are estimated from experimental data has changed, as well. Although the technological advances from single measurement modal parameter estimation to autonomous multiple input, multiple output (MIMO) modal parameter estimation has resulted in improved estimates, the recent developments in autonomous parameter estimation methods has revealed that, while the random errors are reduced, these estimates may still contain small amounts of bias contamination from nearby modes. The results of this contamination are slightly complex estimates of the modal vectors when normal modal vectors are anticipated. The challenge for the analyst is how to deal with this contamination.

In testing situations where modal vectors show some contamination, the problem is often ignored or eliminated through a real normalization procedure of the final modal vectors. Frequently, this process is justified because the contamination appears to be dominantly random. However, when the contamination is biased, this justification becomes uncertain. Even with the most sophisticated modal parameter estimation algorithms and numerical procedures, the form of the contamination will often be biased to look like a nearby mode. This indicates that, while the estimated modal vectors may satisfy whatever algorithm and numerical procedures are being utilized, the estimated modal vectors still contain characteristics that can be perceived as non-physical.

## 2. Background

The estimation of modal vectors in modern modal parameter estimation algorithms normally involves a two-step process. In the first step, the modal participation vectors,  $\{L\}_r$ , are estimated from the eigenvectors of a companion matrix, formulated on the basis of either the short dimension,  $N_s$ , or the long dimension,  $N_L$ , of the measured FRF data matrix. Then in a second step, the corresponding modal vectors,  $\{L\}_r$ , are found from a weighted least squares set of linear equations involving the selected modal frequencies and modal participations from the eigenvalues and eigenvectors of the companion matrix. In modern algorithms, due to the available speed and memory of modern computers used in testing and data analysis, these two steps are often combined, in what appears to the user, as a single step.

The following sections review the relevant theoretical concepts and equations required for discussing the estimation of final, scaled modal vectors. The final scaled modal vectors are often presented as the residues of the partial fraction model of the MIMO FRF data matrix <sup>[1]</sup>. Alternatively, the final, scaled modal vectors can be presented as a vector proportional to the residue vector with associated modal scaling, such as Modal A ( $M_{A_r}$ ).

### 2.1 Modal Vectors from Weighted Estimation of Residues

The equations that relate the complex modal frequencies, complex modal vectors, complex-valued modal participation vectors and residue vectors to the FRF data are well-known and are restated in the following equations for discussion purposes <sup>[1]</sup>:

*Single Reference:*

$$H_{pq}(\omega) = \sum_{r=1}^N \frac{A_{pqr}}{j\omega - \lambda_r} + \frac{A_{pqr}^*}{j\omega - \lambda_r^*} \quad (1)$$

*Multiple Reference:*

$$[H(\omega)] = \sum_{r=1}^N \frac{[A_r]}{j\omega - \lambda_r} + \frac{[A_r^*]}{j\omega - \lambda_r^*} = \sum_{r=1}^{2N} \frac{[A_r]}{j\omega - \lambda_r} \quad (2)$$

$$[H(\omega)]_{N_L \times N_s} = [L]_{N_L \times 2N} \left[ \frac{1}{j\omega - \lambda_r} \right]_{2N \times 2N} [\psi]_{2N \times N_s}^T \quad (3)$$

$$[H(\omega)]_{N_s \times N_L} = [L]_{N_s \times 2N} \left[ \frac{1}{j\omega - \lambda_r} \right]_{2N \times 2N} [\psi]_{2N \times N_L}^T \quad (4)$$

where:

$$A_{pqr} = L_{pr} \psi_{qr} \quad \text{OR} \quad A_{pqr} = \frac{\psi_{pr} \psi_{qr}}{M_{A_r}} \quad (5)$$

In the above equations, and particularly in Equation 5, it should be noted that the residue should be purely imaginary for a normal mode case utilizing displacement over force FRF data. For the anticipated normal mode situation, there is no constraint on the numerical characteristics of either the modal participation coefficient or the modal vector coefficient



However, when these complex-valued vectors are examined closely, the non-dominant portion of the complex-valued vector often correlates very highly with one or more nearby modal vectors. This can be examined by several variants of the MAC calculation and the weighted MAC calculation. This is discussed in the next section and is the subject of a companion paper associated with this work <sup>[6]</sup>.

### 2.2.1 Special Forms of the Modal Assurance Criterion

To understand the nature of the possible modal vector contamination in a complex-valued modal vector, three conventional MAC calculations can be performed (1) between the real parts of the modal vectors and the complex-valued modal vectors (rMAC), (2) between the imaginary parts of the modal vectors and the complex-valued modal vectors (iMAC) and (3) between the real parts of the modal vectors and the imaginary parts of the modal vectors (riMAC). These three MAC calculations and the interpretation of these MAC values will be sensitive to the rotation and normalization of the complex-valued modal vector estimates. The following use and discussion assumes that the complex-valued modal vectors have been rotated so that the central axis of the complex-valued modal vector is centered on the real axis. These three MAC computations identify (1) that the real part of the modal vector is the dominant part of the complex-valued modal vector (rMAC), (2) that the imaginary part of the modal vector is the dominant part of the complex-valued modal vector (iMAC) and (3) that the real and imaginary parts of the modal vector are, or are not, related to one another. All MAC computations in this case are, as always, bounded from zero to one. If near normal modes are expected, (1) the rMAC should be close to one, (2) the iMAC should be close to zero and (3) the riMAC should also be close to zero. Note in the following definitions, complex-valued modal vectors  $c$  and  $d$  can again be any of the modal vectors that the user wishes to include in the evaluation.

$$\text{rMAC}_{cd} = \frac{(\text{Re}\{\psi_c\}^H) \{\psi_d\} \{\psi_d\}^H (\text{Re}\{\psi_c\})}{(\text{Re}\{\psi_c\}^H) (\text{Re}\{\psi_c\}) \{\psi_d\}^H \{\psi_d\}} \quad (7)$$

$$\text{iMAC}_{cd} = \frac{(\text{Im}\{\psi_c\}^H) \{\psi_d\} \{\psi_d\}^H (\text{Im}\{\psi_c\})}{(\text{Im}\{\psi_c\}^H) (\text{Im}\{\psi_c\}) \{\psi_d\}^H \{\psi_d\}} \quad (8)$$

$$\text{riMAC}_{cd} = \frac{(\text{Re}\{\psi_c\}^H) (\text{Im}\{\psi_d\}) (\text{Im}\{\psi_d\}^H) (\text{Re}\{\psi_c\})}{(\text{Re}\{\psi_c\}^H) (\text{Re}\{\psi_c\}) (\text{Im}\{\psi_d\}^H) (\text{Im}\{\psi_d\})} \quad (9)$$

The above MAC evaluations identify whether, and how, the contamination of a complex-valued modal vector is related to another of the identified modal vectors. However, the MAC computation is normalized to unity vector length, vector by vector, for the vectors used in the calculation. A weighted MAC can be used to determine the degree or scale of the contamination. The following three definitions of the weighting for each of the above MAC calculations limits the associated MAC value to a fraction of the zero to one scale. If near normal modes are expected, (1) the weighting and rwMAC should be close to one, (2) the weighting and iwMAC should be close to zero and (3) the combined weighting and riwMAC should also be close to zero. Note in the following definitions, complex-valued modal vectors  $c$  and  $d$  can again be any of the modal vectors that the user wishes to include in the evaluation.

$$\text{rwMAC}_{cd} = \text{rW}_c \times \text{rMAC}_{cd} \quad \text{where } \text{rW}_c = \frac{(\text{Re}\{\psi_c\}^H) (\text{Re}\{\psi_c\})}{\{\psi_c\}^H \{\psi_c\}} \quad (10)$$

$$\text{iwMAC}_{cd} = \text{iW}_c \times \text{iMAC}_{cd} \quad \text{where } \text{iW}_c = \frac{(\text{Im}\{\psi_c\}^H) (\text{Im}\{\psi_c\})}{\{\psi_c\}^H \{\psi_c\}} \quad (11)$$

$$\text{riwMAC}_{cd} = \text{rW}_c \times \text{iW}_d \times \text{riMAC}_{cd} \quad (12)$$

### 2.3 Modal Vector Contamination - Simple Example

For the following example, the presentation is illustrative of the nature and appearance of the complex modal vector contamination. It is not a rigorous definition of the specific form and source of contamination that results from the solution of the companion matrix.

For the basic partial fraction model, the numerator or residue will be a purely imaginary number for the case of a normal mode, assuming that the FRF is in displacement over force form. The residue for all modes in the summation will also be plus/minus purely imaginary numbers.

$$\{H(\omega)\} = \sum_{r=1}^{2N} \frac{\{A\}_r}{j\omega - \lambda_r} \quad (13)$$

Assuming that the numerical solution procedure does not completely eliminate the estimate of one residue from the next, the question is then, *what will be the nature of the contamination?* For mode  $r$ , the residue  $A_{pqr}$  for a particular measurement  $H_{pq}$  will be a purely imaginary number but, if there is contamination coming from the next mode higher (or lower) in frequency, this will alter the desired residue  $A_{pqr}$ , adding both real and imaginary contamination coming from mode  $s$  in the following way:

$$\left\{ \hat{A} \right\}_r = \{A\}_r + \frac{\{A\}_s}{j\omega_r - \lambda_s} = \{A\}_r + \frac{\{A\}_s}{\sigma_s + j(\omega_r - \omega_s)} \quad (14)$$

Even if the nearby residue is also purely imaginary, the contamination of the  $A_{pqr}$  will be biased in both the real and imaginary part by a contribution that is proportional to the nearby mode. Due to the magnitude of the imaginary part of  $A_{pqr}$  this contribution may not be noticeable but, as the real part of the residue  $A_{pqr}$  should be zero, the contamination of the real part of the residue will be quite noticeable. This was demonstrated in two recent papers [6,10] and the form of this contamination has been known for some time [7].

### 3. Normalization of the Modal Weighting (Participation) Vector

Identifying the potential contamination of modal vectors is helpful to the thorough understanding of modal parameter estimation algorithms and autonomous procedures, as well as, being instructive for potential removal of the contamination. If some sort of real normalization is desirable (to match up well with an undamped, analytical model, for example), understanding of the contamination that is being removed is a prerequisite to any procedure. Random contamination may simply be ignored, smoothed or averaged out, but if the contamination is related to nearby modes, it may indicate that the modal parameter estimation may need further evaluation or that more data from additional reference DOFs is required.

#### 3.1 Central Axis Rotation

In order to establish a uniform procedure for normalizing the modal participation vector which will be used as the weighting vector when estimating modal vectors from MIMO FRF data, each potentially complex valued vector must first be rotated to an orientation where the dominant information of the vector in complex space is aligned with the real axis. This is required since the vector is the result of the solution of an eigenvalue-eigenvector problem involving the complex-valued MIMO FRF data.

Given an original (contaminated) modal participation vector for mode  $r$ , a central axis rotation method is utilized to determine the dominant axes. These dominant axes can be identified via the singular value decomposition of the relationship between the real part,  $\{L_R\}_r$ , and imaginary part,  $\{L_I\}_r$ , of the modal participation vector for mode  $r$  as follows:

$$[U, \Sigma, V] = \text{svd} \left( \begin{bmatrix} \{L_I\}_r & \{L_R\}_r \end{bmatrix}^T \begin{bmatrix} \{L_I\}_r \\ \{L_R\}_r \end{bmatrix} \right) \quad (15)$$

Recognize that this decomposition is an attempt to locate the two dominant axes of a 2-D ellipse that encompasses the modal participation vector data in the complex plane. Following the decomposition, the central axis angle is estimated using the true (four quadrant) arctangent of the right singular vector relationship. Note that, regardless of the number of DOF positions represented in the modal vector, the right singular vector matrix will always be two by two in dimension representing the 2-D characteristics of the ellipse.

$$\bar{\phi}_r = \tan^{-1} \left( \frac{V_{22}}{-V_{12}} \right) \quad (16)$$

After identifying the central axis angle, the original complex vector is rotated by multiplying by the complex rotational phasor.

$$\left\{ \hat{L} \right\}_r = \left( \cos(\bar{\phi}_r) - j \sin(\bar{\phi}_r) \right) \{L\}_r \quad (17)$$

This rotation and normalization procedure assures that the resulting vector is dominantly real, based upon all of the vector information, rather than a single DOF that is chosen arbitrarily (for example, rather than selecting the DOF associated with the largest modal vector coefficient).

### 3.2 Modal Vector Complexity

Modal vector complexity is often defined in terms of mean phase deviation as an indication of how the phase deviates from zero and/or 180 degrees. This definition allows some ambiguity in what is meant by a *complex mode*. It may simply mean that the elements of the estimated modal vector contain complex values. For this case, the elements of the modal vector may be rotated by an angle in the complex plane, but are otherwise colinear. Or it may mean that the modal vector contains complex values that cannot be made real by a simple complex phasor rotation. For this case, the modal coefficients are not all colinear in the complex plane. For this development, it is the second definition that is used.

The mean phase deviation ( $MPD_r$ ) for modal vector  $r$  has been defined historically as a number between zero and unity where zero represents a real valued modal vector (normal mode) and where unity represents a complex valued modal vector with no recognizable dominant real or imaginary characteristic, once an attempt has been made to rotate the vector to a dominant central axis position. This fraction is often multiplied by 100 to represent the percentage of complex valued modal vector characteristics. In terms of the definitions utilized in the previous section, assuming that the modal vector has already been rotated to its most dominant real orientation, the  $MPD_r$  is defined as the norm of the imaginary part of the rotated vector divided by the norm of the real part of the rotated vector, as shown in Equation 18. Thus, the  $MPD_r$  gives a dispersion ratio around the central axis of the rotated modal vector bounded between zero and one.

*Mean Phase Deviation ( $MPD_r$ ):*

$$MPD_r = \frac{\left\| \left\{ \hat{\psi}_I \right\}_r \right\|}{\left\| \left\{ \hat{\psi}_R \right\}_r \right\|} \quad (18)$$

Once the  $MPD_r$  is defined in terms of the fraction between zero and unity, the associated mean phase correlation for modal vector  $r$  is defined as in Equation 19.

*Mean Phase Correlation ( $MPC_r$ ):*

$$MPC_r = 1 - MPD_r \quad (19)$$

The mean phase correlation can then be interpreted as an indicator of normalcy; from a purely normal mode (1.0) to a purely complex mode (0.0).

### 3.3 Proposed New Methodology

The proposed new methodology involves a real normalization of the modal participation vectors,  $\left\{ L_{pr} \right\}$ , that are used as the weighting factors in the corresponding estimates of the modal vectors  $\left\{ \psi_{qr} \right\}$ . No limitation or normalization is placed upon the modal vectors  $\left\{ \psi_{qr} \right\}$ . In this way, the final residue vector  $\left\{ A_{pqr} \right\}$  is still estimated as a completely complex valued vector as noted in Equation 5. The real normalization of the modal participation vectors  $\left\{ L_{pr} \right\}$  currently is implemented by dropping the imaginary part of the modal participation vectors  $\left\{ L_{pr} \right\}$  after the vectors have been rotated to the most dominant central axis as defined in Equations 15-17.

This simple procedure does not eliminate complex-valued modal vectors when they exist due to non-proportional damping but shows dramatic improvement in the estimation of the residue vectors when the structure is thought to satisfy the

conditions of proportional damping (normal modes). In these cases, the product of the modal participation vectors and the modal vectors, as noted in Equation 5, yields residues that are very close to purely imaginary vectors as would be expected for the normal mode case involving displacement over force FRF data. The next two sections demonstrate these characteristics. The academic example shows that the real normalization of the modal participation vectors has no negative effects on the estimation of the expected final modal vectors while the practical example indicates that for a case where modal contamination has been noted, the real normalization of the modal participation vectors greatly reduces this observed phenomena.

#### 4. 15 DOF Analytical Example

A 15 DOF analytical example is used to generate a set of MIMO FRFs with known properties to be certain that the real normalization procedure gives expected results in the two cases. Three different cases were utilized to perform this evaluation. Case I involved a proportionally damped model, Case II involved a non-proportionally damped model (5 percent complexity) and Case III involved a non-proportionally damped model (20 percent complexity).

To clarify the three cases in terms of the previous modal vector complexity concepts, the percentage of non-proportional damping (NPD) utilized the  $MPD_r$  as a descriptor metric, multiplied times 100 to give the result in percentage form. For proportional damping (PD) used in Case I, the  $MPD_r$  for the vectors was essentially zero when a small amount of random noise was included. For Case II where the non-proportional damping is described as 5% NPD, the complexity of the analytical vectors was nominally around 5% MPD. For Case III where the non-proportional damping is described as 20% NPD, the complexity of the analytical vectors was nominally around 20% MPD. For comparison, a 100% NPD would be 100% MPD implying that the vector is completely complex and there is no central vector at all.

The comparison of the three cases is presented in Figure 2. The left column is the real weighting and the right column is the complex weighting for each case. As can be noted, no significant difference exists between the cases. A comparison of the resultant estimated poles and vectors with the MCK analytical values reveals that the estimation of complex vectors using real weighting is essentially the same, differing only by very small amounts that can be related to the random noise that has been added to the synthesized FRF data.

The conclusion that can be drawn from Figure 2, as well as inspecting the final modal frequencies and modal vectors that are estimated from these consistency diagrams, is that the real normalization of the modal participation vector that is used as a weighting vector appears to have no impact on getting the correct modal vector, regardless of proportional or non-proportional damping.

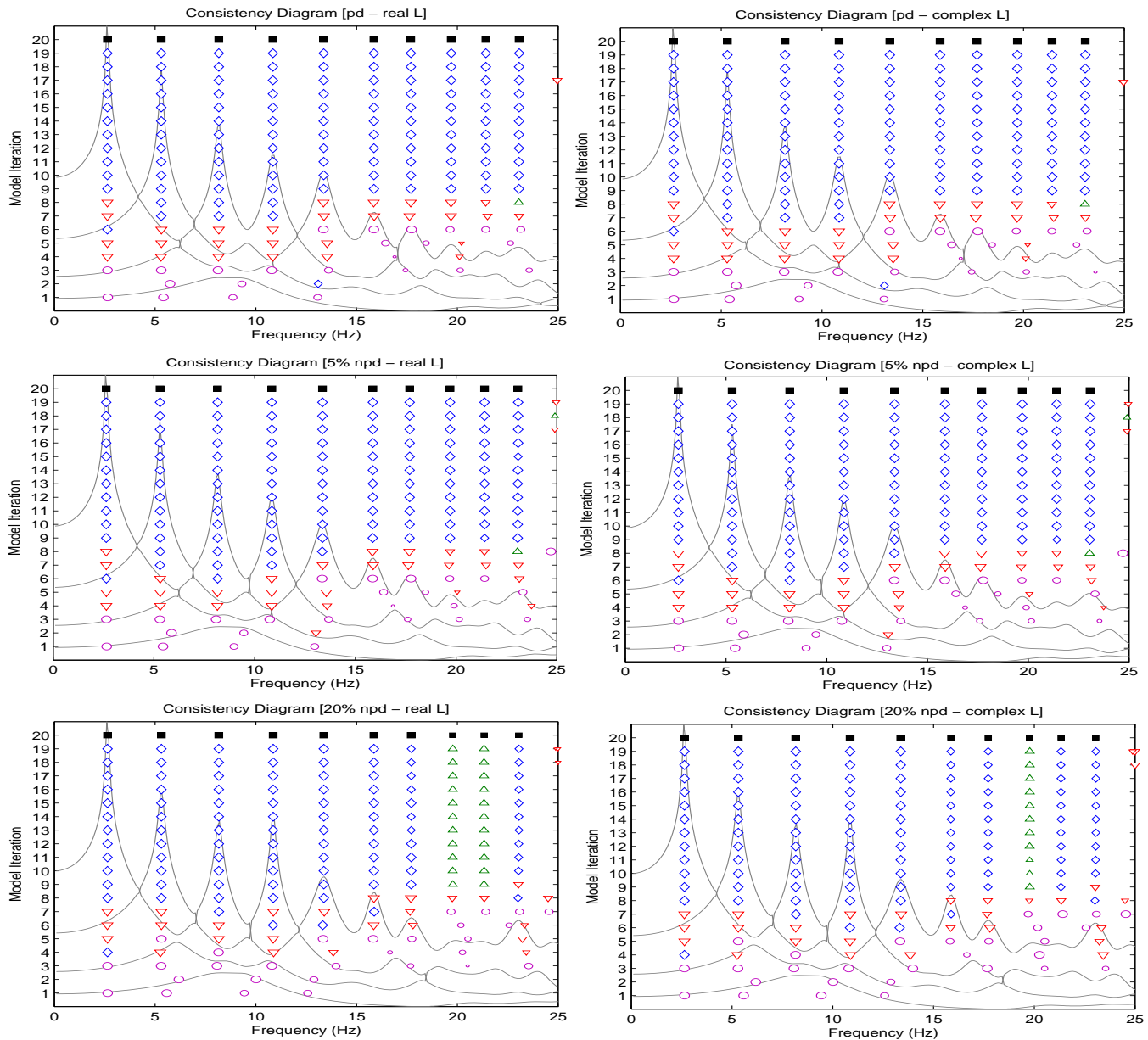


**Figure 2.** 15 DOF Consistency Diagram, Real and Complex Weighting, Proportional and Non-Proportional Damping

### 5. C-Plate Example

The data used for the following section is MIMO FRF data taken from an impact test of a steel disc supported in a pseudo free-free boundary condition. The steel disc is approximately 2 cm. thick and 86 cm. in diameter with several small holes through the disc. The center area of the disc (diameter of approximately 25 cm.) has a thickness of approximately 6 cm. There are seven reference accelerometers and measured force inputs from an impact hammer are applied to thirty-six locations, including next to the seven reference accelerometers. The frequency resolution of the data is 5 Hertz. While the disc is not as challenging as some industrial data situations that contain more noise or other complicating factors like small nonlinearities, the disc has a number of pseudo-repeated roots spaced well within the 5 Hertz frequency resolution and a mix of close modes involving repeated and non-repeated roots which are very challenging. Based upon the construction of the disc, real-valued, normal modes can be expected and the inability to resolve these modes can be instructive relative to both modal parameter estimation algorithm and autonomous procedure performance. For the interested reader, a number of realistic examples are shown in other past papers including FRF data from an automotive structure and a bridge structure [8-9]



### 5.1 C-Plate Example: Estimates with Complex Weighting

For this example, the entire frequency range from 200 Hz to 2500 Hz was fit by the Rational Fraction Polynomial Algorithm with Z-frequency weighting (RFP-Z) in a single parameter estimation run using traditional complex participation weighting. The CSSAMI autonomous modal parameter estimation procedure was utilized to remove user bias from the selected results [8-10] using the same input parameters to the RFP-z algorithm and the CSSAMI procedure. The following results are similar regardless of the base modal parameter estimation algorithm chosen.

It can be observed in the MAC plot (Figure 3) that there exists a coupling contamination between the 2300 Hz repeated root modes. This is further revealed by the symbols in the consistency diagram (Figure 4) where the green delta symbol indicates that no stable pole and vector was identified. In addition, the small size of the symbol indicates that the vector that has been found is significantly complex-valued. Using the weighted and unweighted versions of the riMAC (Figure 5), it is evident that each of the repeated root pairs has some contamination from its twin. Finally, expanding the region of the consistency diagram around the 2300 Hz modal pair (Figure 6), it is clear that while a consistent frequency and damping are identified, there is no consistent modal vector identified from iteration to iteration.

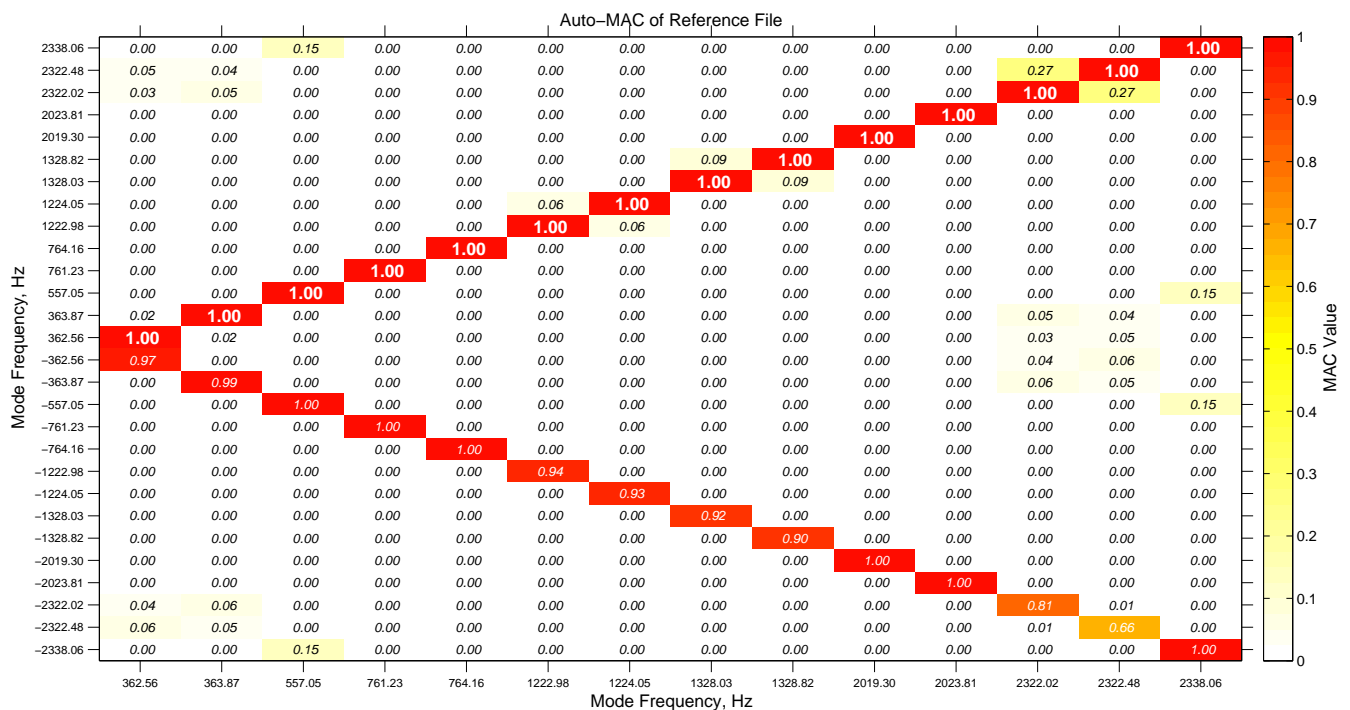
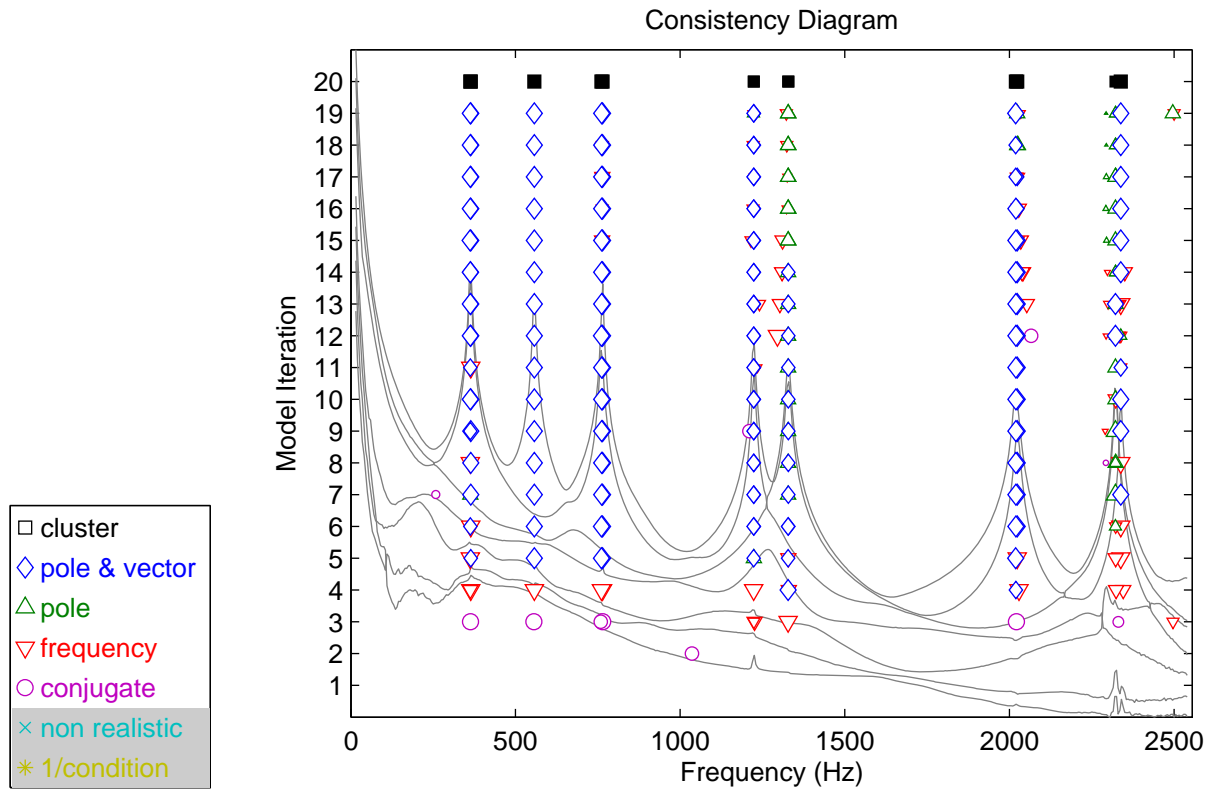
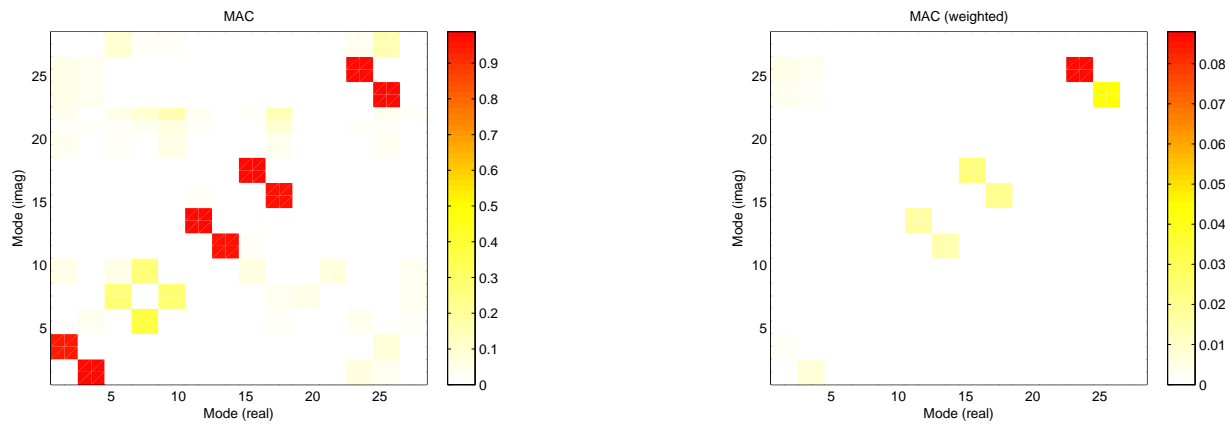


Figure 3. C-Plate MAC of Modal Vectors and Conjugate Modal Vectors - Complex Weighting



**Figure 4.** C-Plate Consistency Diagram, Complex Weighting, Full Frequency Range



**Figure 5.** C-Plate, Complex Weighting, riMAC and riwMAC

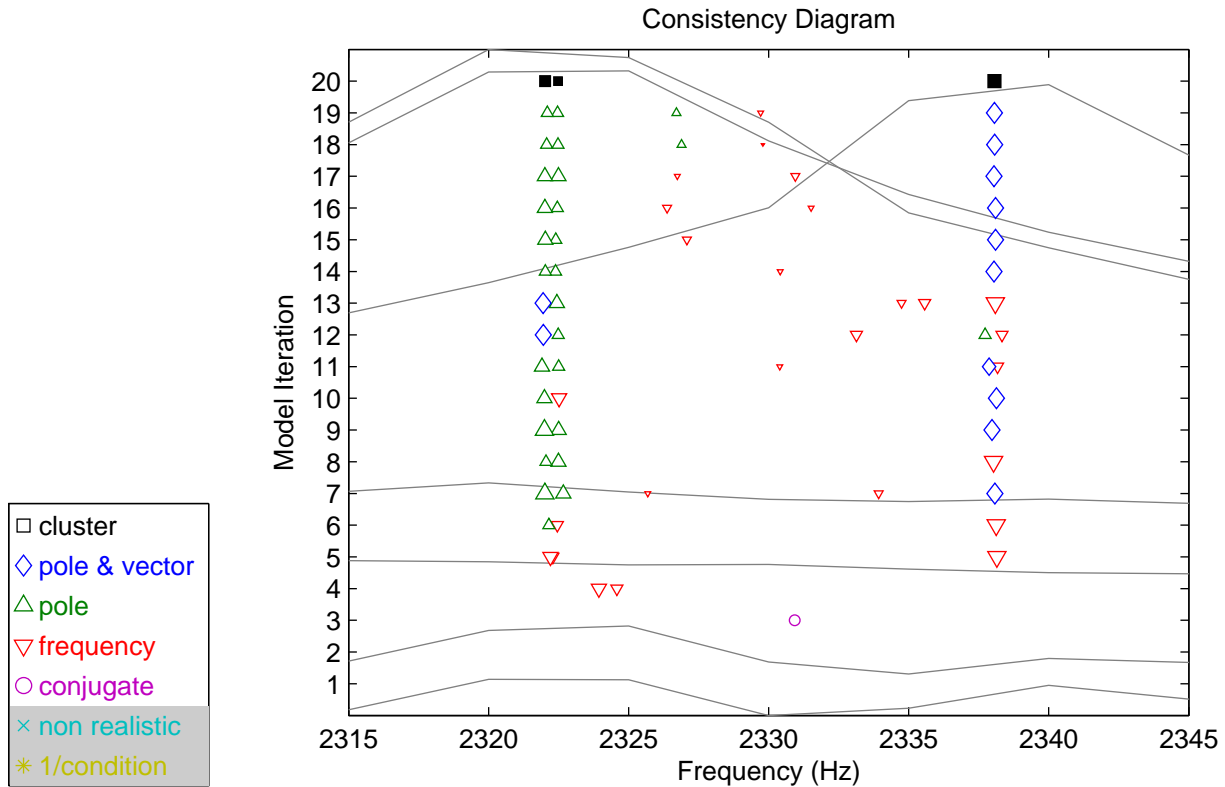


**Figure 6.** C-Plate Consistency Diagram, Complex Weighting, 2315-2345 Hz. Range

While this solution represents the theoretical concept of generalized weighting vectors for each mode that can be complex-valued, the results for this case yield solutions that are slightly non-physical when the nature of the structure under test is considered.

### 5.2 C-Plate Example: Estimates with Real Weighting

For this example, the entire frequency range from 200 Hz to 2500 Hz was again fit by the Rational Fraction Polynomial Algorithm with Z-frequency weighting (RFP-z) in a single parameter estimation run. The final results were again determined from the CSSAMI autonomous procedure. All conditions match the modal parameter estimation process used in the last section. This time, however, instead of using the complex valued modal participation vectors as weighting vectors, real normalization of the modal participation vector (first rotated to its dominant central axis) was used to generated real-valued weighting vectors.

Dramatically improved results can be observed in the following figures. It can be observed in the MAC plot (Figure 7) that the coupling contamination between the 2300 Hz repeated root modes has been eliminated. Further, it can be observed that the cross MAC between each vector and its complex conjugate is also improved. This improvement is further revealed by the symbols in the consistency diagram (Figure 8). Whereas before the symbols indicated a complex-valued, inconsistent modal vector, in this case, the large blue diamonds indicate a consistent, nearly normal mode. The nearly two orders of magnitude change in the weighted riMAC (Figure 9), also indicates the significant reduction in contamination. Finally, expanding the region of the consistency diagram around the 2300 Hz modal pair (Figure 10), it is clear that both the pole and the modal vector are identified consistently from iteration to iteration.

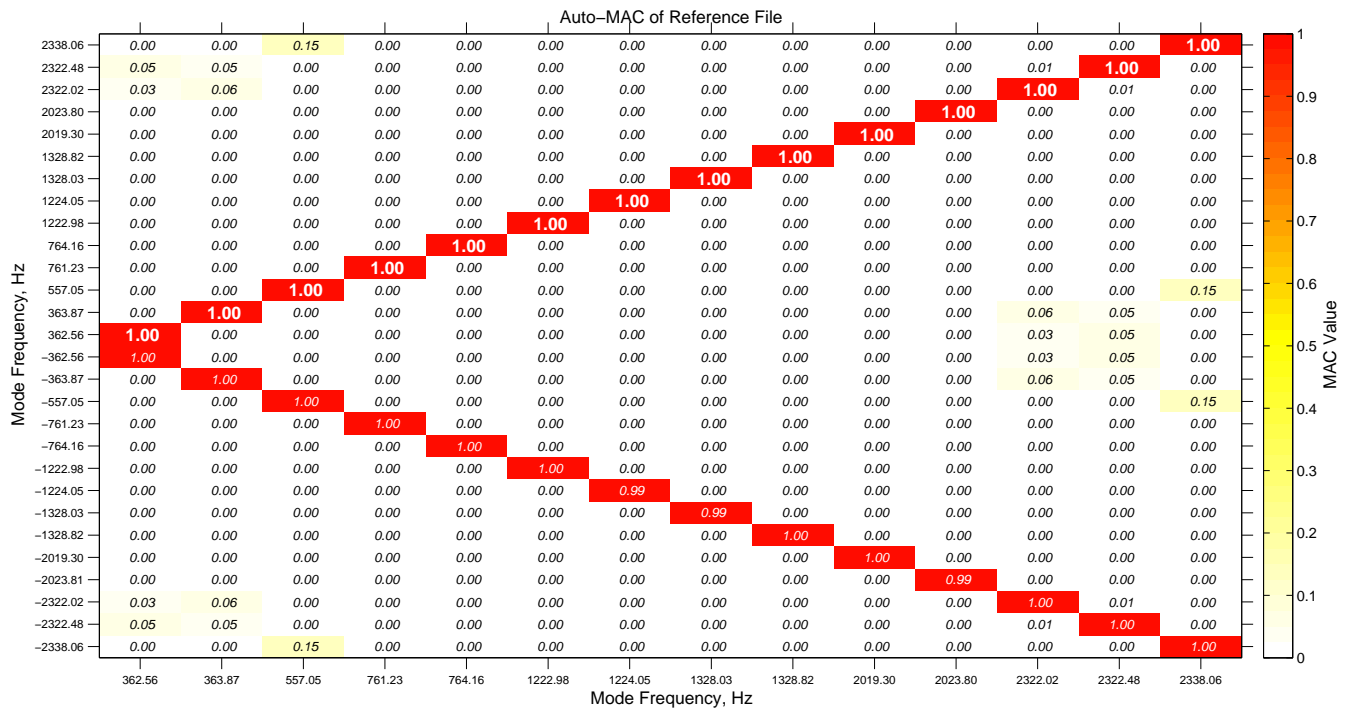


Figure 7. MAC of Modal Vectors and Conjugate Modal Vectors - Real Weighting

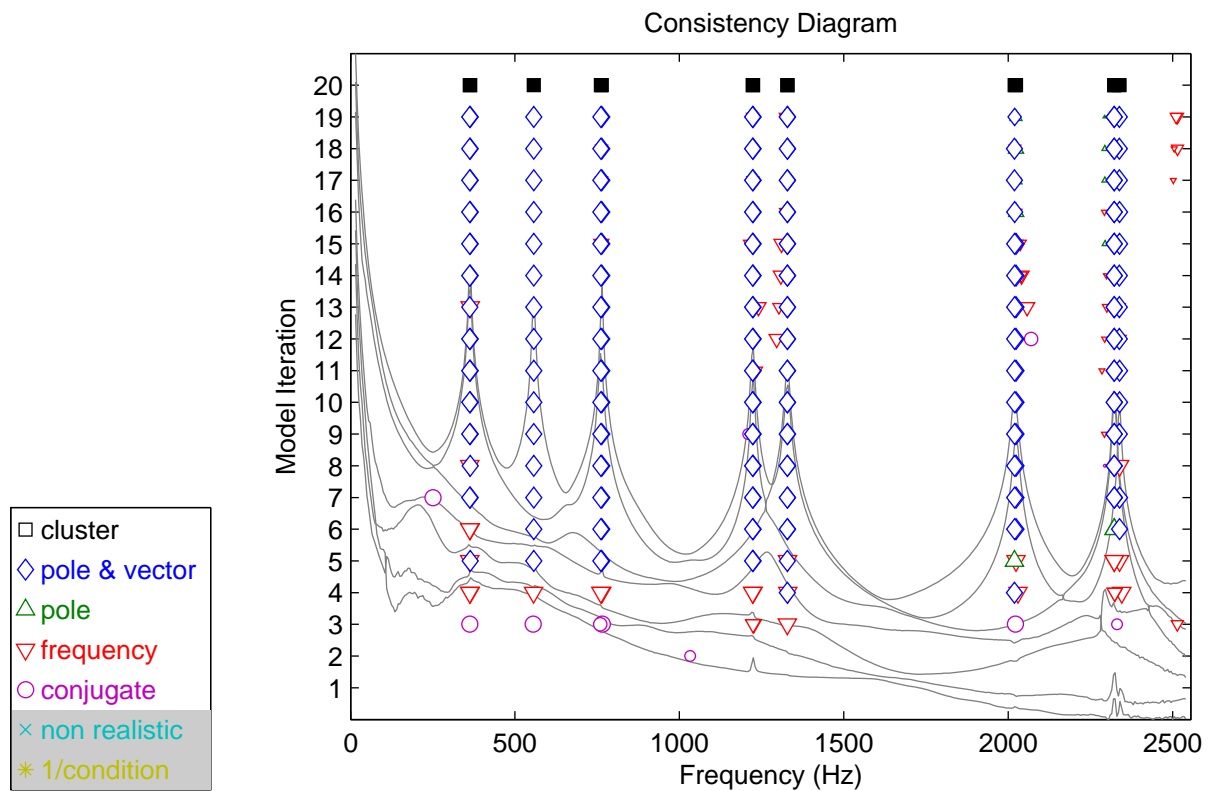
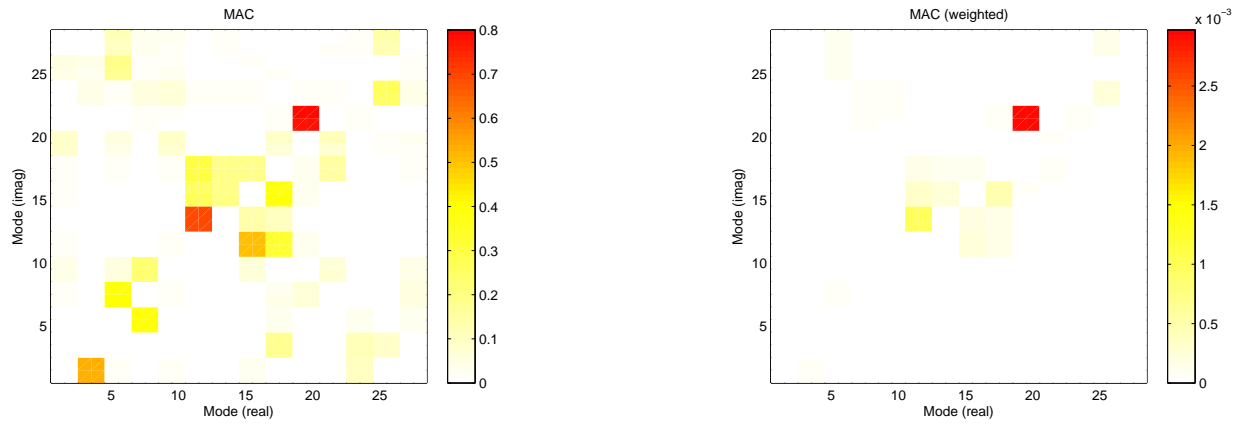
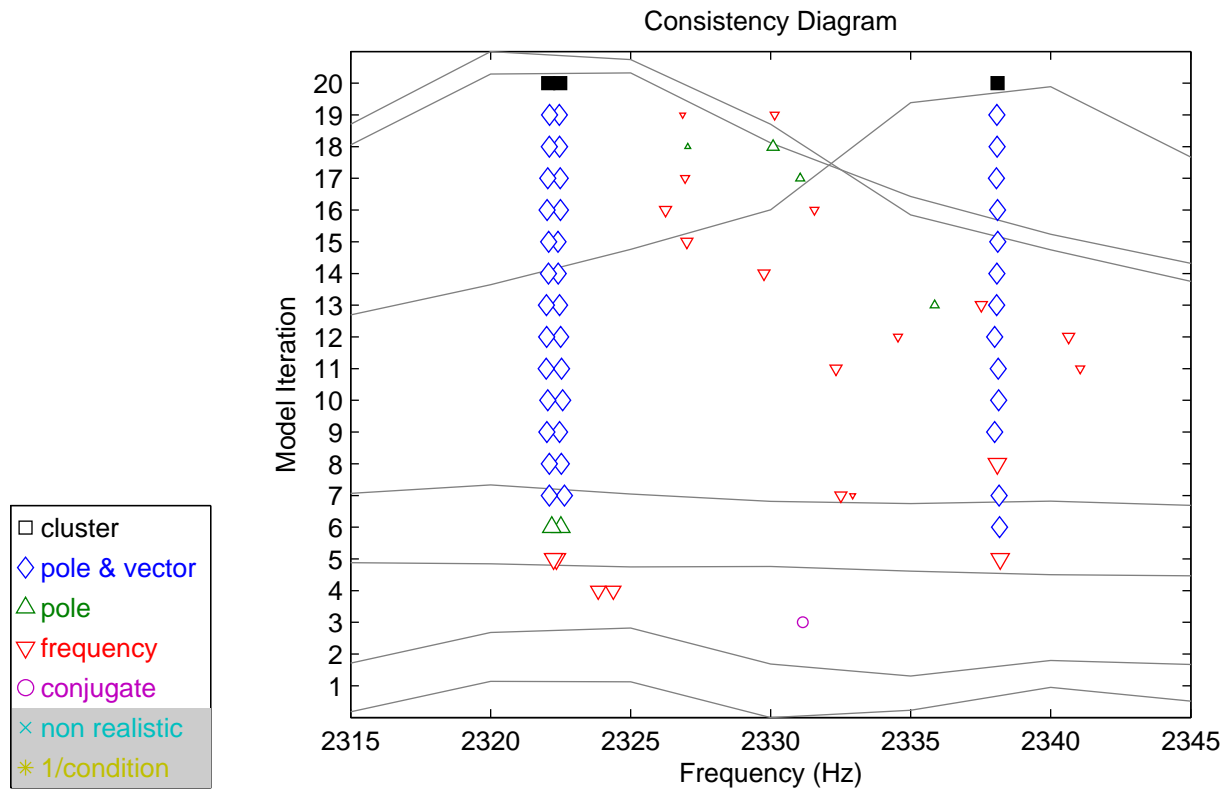


Figure 8. C-Plate Consistency Diagram, Real Weighting, Full Frequency Range



**Figure 9.** C-Plate, Real Weighting, riMAC and riwMAC"



**Figure 10.** C-Plate Consistency Diagram, Real Weighting, 2315-2345 Hz Range

## 6. Summary And Future Work

A relatively simple change to the weighting vectors used in the weighted estimation of the residues for each mode has dramatically improved the results with little to no observable negative effects. For the examples chosen, the use of central vector rotation and real normalization of the modal participation vectors appears to improve the quality and characteristics of the final, scaled modal vectors (residues) significantly.

Future work will involve alternative numerical methods for decoupling the contaminated modal vectors and a more rigorous evaluation of the source of contamination derived from the companion matrix solution with the goal of eliminating the

contamination earlier in the parameter estimation process. A more complete understanding of why this technique works so well is still needed.

### **Acknowledgements:**

The authors would like to acknowledge the collaboration and assistance from the graduate students and faculty of the Structural Dynamics Research Lab at the University of Cincinnati. In particular, the discussions and collaborations with Dr. David L. Brown have been instrumental in the progress made to this point.

### **7. References**

- [1] Allemang, R.J., Phillips, A.W., "The Unified Matrix Polynomial Approach to Understanding Modal Parameter Estimation: An Update", Proceedings, International Conference on Noise and Vibration Engineering (ISMA), 2004.
- [2] Allemang, R. J., Brown, D.L., "A Correlation Coefficient for Modal Vector Analysis", Proceedings, International Modal Analysis Conference, pp.110-116, 1982.
- [3] Heylen, W., "Extensions of the Modal Assurance Criterion", Journal of Vibrations and Acoustics, Vol. 112, pp. 468-472, 1990.
- [4] Lallement, G., Kozanek, J., "Comparison of Vectors and Quantification of their Complexity", Proceedings, International Modal Analysis Conference, pp. 785-790, 1999.
- [5] "The Modal Assurance Criterion (MAC): Twenty Years of Use and Abuse", Allemang, R.J., Proceedings, International Modal Analysis Conference, pp. 397-405, 2002. *Sound and Vibration Magazine*, Vol. 37, No. 8, pp. 14-23, August, 2003.
- [6] Allemang, R.J., Phillips, A.W., "Un-weighted and Weighted Versions of the Modal Assurance Criterion (MAC) for Evaluation of Modal Vector Contamination", Proceedings, International Modal Analysis Conference (IMAC), 8 pp., 2014.
- [7] Deblauwe, F., Allemang, R.J., "A Possible Origin of Complex Modal Vectors", Proceedings, 11th International Seminar on Modal Analysis (ISMA), Katholieke Universiteit Leuven, Belgium, 10 pp., 1986.
- [8] Phillips, A.W., Allemang, R.J., Brown, D.L., "Autonomous Modal Parameter Estimation: Methodology", Proceedings, International Modal Analysis Conference (IMAC), 22 pp., 2011.
- [9] Allemang, R.J., Phillips, A.W., Brown, D.L., "Autonomous Modal Parameter Estimation: Statistical Considerations", Proceedings, International Modal Analysis Conference (IMAC), 17 pp., 2011.
- [10] Allemang, R.J., "Spatial Information in Autonomous Modal Parameter Estimation", Invited Keynote Paper, International Conference on Structural Engineering Dynamics (ICEDyn 2013), Sesimbra, Portugal, 18 pp, June 2013.